

Coordination Modes of Boranes in Polyhydride Ruthenium Complexes: σ -Borane versus Dihydridoborate

Sébastien Lachaize,[†] Khaled Essalah,^{‡,§} Virginia Montiel-Palma,^{†,||}
Laure Vendier,[†] Bruno Chaudret,[†] Jean-Claude Barthelat,[‡] and
Sylviane Sabo-Etienne^{*,†}

Laboratoire de Chimie de Coordination du CNRS, 205 route de Narbonne, 31077 Toulouse Cedex 04, France, and Laboratoire de Physique Quantique, IRSAMC/UMR 5626, Université Paul Sabatier, 118 route de Narbonne, 31062 Toulouse Cedex 04, France

Received April 11, 2005

The bis(dihydrogen) complex $\text{RuH}_2(\eta^2\text{-H}_2)_2(\text{PCy}_3)_2$ (**1**) reacts at room temperature with 1 equiv of either HBpin or HBcat to produce the σ -borane complexes $\text{RuH}_2(\eta^2\text{-HBpin})(\eta^2\text{-H}_2)(\text{PCy}_3)_2$ (**2Bpin**) and $\text{RuH}_2(\eta^2\text{-HBcat})(\eta^2\text{-H}_2)(\text{PCy}_3)_2$ (**2Bcat**), respectively, by substitution of one $\sigma\text{-H}_2$ ligand by one $\sigma\text{-B-H}$. In contrast, when using the 9-BBN reagent, the dihydridoborate complex $\text{RuH}[(\mu\text{-H})_2\text{BBN}](\eta^2\text{-H}_2)(\text{PCy}_3)_2$ (**2BBN**) is formed. The coordination modes of the borane ligands have been ascertained by NMR spectroscopy, X-ray diffraction, and theoretical studies (DFT/B3LYP). The results indicate that the dialkoxyborane ligands (HBpin and HBcat) are not acidic enough to stabilize a “true” symmetrical dihydridoborate coordination mode. They thus lead to σ -borane complexes presenting a small H/BH cis interaction between the boron atom and the adjacent hydride. The $\sigma\text{-H}_2$ ligand in **2Bpin** is located by X-ray diffraction at 90 K and found to be perpendicular to the equatorial plane. DFT calculations lead to the optimization of the two degenerate isomers $\text{RuH}_2[\eta^2\text{-HB}(\text{OCH}_2)_2](\eta^2\text{-H}_2)(\text{PMe}_3)_2$ (**5Bpin_a**) (analogous to **2Bpin**) and $\text{RuH}[(\mu\text{-H})_2\text{B}(\text{OCH}_2)_2](\eta^2\text{-H}_2)(\text{PMe}_3)_2$ (**5Bpin_b**), demonstrating that $\sigma\text{-H}_2$ rotation and σ -borane versus dihydridoborate ligation are intimately correlated. In contrast, the 9-BBN reagent is a strong Lewis acid and leads to a dihydridoborate complex. The theoretical study on $\text{RuH}[(\mu\text{-H})_2\text{Bpin}](\eta^2\text{-HBpin})(\text{PCy}_3)_2$ (**3Bpin**) shows that the bonding is also dependent on the hydride basicity: the $\text{RuH}[(\mu\text{-H})_2\text{B}(\text{OCH}_2)_2](\text{PMe}_3)_2$ fragment used as a model for $\text{RuH}[(\mu\text{-H})_2\text{Bpin}](\text{PCy}_3)_2$ is not basic enough to contain a second ligand bound in a dihydridoborate mode, despite the stabilization that should be gained from the resulting symmetrical structure.

Introduction

The past decade has seen major conceptual advances in the field of borane activation.¹ Landmark findings have been disclosed both in fundamental aspects of coordination chemistry and in catalysis.^{2–4} Several reports have shown that boron-containing moieties can adopt several geometries when bound to both early-⁵ and late-transition-metal centers⁶ that also support hydride ligands (see Figure 1). Better knowledge has

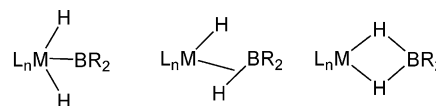


Figure 1. Possible structures resulting from the coordination of HBR_2 on the L_nMH fragment.

been gained on the properties of transition-metal boryl compounds,^{6a} and isolation of a few σ -borane complexes has been achieved following the first report in 1996 by Hartwig et al.^{7–11} These two classes of compounds play

* To whom correspondence should be addressed. E-mail: sabo@lcc-toulouse.fr.

[†] LCC-CNRS.

[‡] IRSAMC.

[§] Permanent address: IPEST, 2070 La Marsa, Tunisia.

^{||} Permanent address: CIQ, Universidad Autónoma del Estado de Morelos, Cuernavaca, Morelos 62210, México.

(1) Kubas, G. J. *Metal Dihydrogen and σ -Bond Complexes*; Kluwer Academic/Plenum Publishers: New York, 2001.

(2) Burgess, K.; Ohlmeyer, M. J. *Chem. Rev.* **1991**, *91*, 1179.

(3) Smith, M. R., III. *Prog. Inorg. Chem.* **1999**, *48*, 505.

(4) Braunschweig, H.; Colling, M. *Coord. Chem. Rev.* **2001**, *223*, 1.

(5) (a) Hartwig, J. F.; De Gala, S. R. *J. Am. Chem. Soc.* **1994**, *116*, 3661. (b) Lantero, D. R.; Motry, D. H.; Ward, D. L.; Smith, M. R., III. *J. Am. Chem. Soc.* **1994**, *116*, 10811. (c) Lantero, D. R.; Miller, S. L.; Cho, J. Y.; Ward, D. L.; Smith, M. R., III. *Organometallics* **1999**, *18*, 235. (d) Liu, D.; Lam, K.-C.; Lin, Z. *J. Organomet. Chem.* **2003**, *680*, 148. (e) Pandey, K. K. *Inorg. Chem.* **2001**, *40*, 5092.

(6) (a) Irvine, G. J.; Lesley, M. J. G.; Marder, T. B.; Norman, N. C.; Rice, C. R.; Robins, E. G.; Roper, W. R.; Whittell, G. R.; Wright, L. J. *Chem. Rev.* **1998**, *98*, 2685. (b) Baker, R. T.; Ovenall, D. W.; Calabrese, J. C.; Westcott, S. A.; Taylor, N. J.; Williams, I. D.; Marder, T. B. *J. Am. Chem. Soc.* **1990**, *112*, 9399. (c) Westcott, S. A.; Marder, T. B.; Baker, R. T.; Calabrese, J. C.; Harlow, R. L.; Lam, K. C.; Lin, Z. *Polyhedron* **2004**, *23*, 2665.

(7) Hartwig, J. F.; Muhoro, C. N.; He, X.; Eisenstein, O.; Bosque, R.; Maseras, F. *J. Am. Chem. Soc.* **1996**, *118*, 10936.

(8) Muhoro, C. N.; Hartwig, J. F. *Angew. Chem., Int. Ed.* **1997**, *36*, 1510.

(9) Muhoro, C. N.; He, X.; Hartwig, J. F. *J. Am. Chem. Soc.* **1999**, *121*, 5033.

(10) Schlecht, S.; Hartwig, J. F. *J. Am. Chem. Soc.* **2000**, *122*, 9435.

(11) Montiel-Palma, V.; Lumbierres, M.; Donnadiou, B.; Sabo-Etienne, S.; Chaudret, B. *J. Am. Chem. Soc.* **2002**, *124*, 5624.

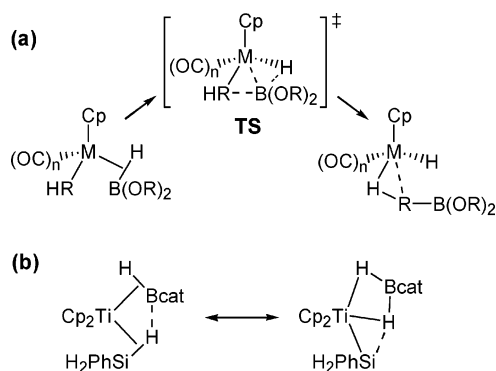


Figure 2. (a) Proposed σ -bond metathesis step in $\text{CpM}(\text{RH})(\text{CO})_n[\text{HB}(\text{OR})_2]$ ($\text{R} = \text{CH}_2$; $\text{M} = \text{Fe}$, $n = 2$; $\text{M} = \text{W}$, $n = 1$). (b) Representation of the two possible mesomers of $\text{Cp}_2\text{Ti}(\eta^2\text{-HBcat})(\eta^2\text{-HSiH}_2\text{Ph})$.

a central role in key events in catalysis, such as B–H oxidative addition and reductive elimination steps. New applications overcoming the well-known hydroboration process have been disclosed. Borane activation by transition-metal complexes now holds promise as a way to selectively functionalize alkanes and arenes. Ishiyama and Miyaura have reviewed the most recent developments in that field.^{12–18} The formation of an intermediate with a strong but reactive C–B bond is indeed a method of choice to functionalize alkanes.^{19,20} Hartwig et al. have recently proposed a mechanism for alkane borylation in which a σ -borane ligand is directly implied in a σ -bond metathesis step (see Figure 2a).²¹ In this case, the Lewis acidity of the boron atom plays a major role in the interaction with the adjacent alkyl ligand. A separate work shows that the mixed borane–silane complex $\text{Cp}_2\text{Ti}(\eta^2\text{-HBcat})(\eta^2\text{-HSiH}_2\text{Ph})$, presenting an interaction between the Si–H bond and the boron atom,⁹ can be seen as a model for C–H bond activation assisted by a σ -borane. A dihydridoborate silyl species appears to be a possible resonance form (see Figure 2b). Lin et al. have shown by theoretical calculations that the same behavior could be expected with CH_4 , the Lewis acidity of the boron atom playing again a key role.²²

Our group has recently reported that the bis(dihydrogen) complex $\text{RuH}_2(\eta^2\text{-H}_2)_2(\text{PCy}_3)_2$ (**1**) reacts with excess HBpin to give a complex with two borane ligands

(12) Ishiyama, T.; Miyaura, N. *J. Organomet. Chem.* **2003**, *680*, 3.

(13) Ishiyama, T.; Takagi, J.; Ishida, K.; Miyaura, N.; Anastasi, N. R.; Hartwig, J. F. *J. Am. Chem. Soc.* **2002**, *124*, 390.

(14) Lawrence, J. D.; Takahashi, M.; Bae, C.; Hartwig, J. F. *J. Am. Chem. Soc.* **2004**, *126*, 15334.

(15) Cho, J.-Y.; Iverson, C. N.; Smith, M. R., III. *J. Am. Chem. Soc.* **2000**, *122*, 12868.

(16) Cho, J.-Y.; Tse, M. K.; Holmes, D.; Maleczka, R. E., Jr.; Smith, M. R., III. *Science* **2002**, *295*, 305.

(17) Shimada, S.; Batsanov, A. S.; Howard, J. A. K.; Marder, T. B. *Angew. Chem., Int. Ed.* **2001**, *40*, 2168.

(18) Lam, W. H.; Lam, K. C.; Lin, Z.; Shimada, S.; Perutz, R. N.; Marder, T. B. *Dalton* **2004**, 1556.

(19) Jones, W. D. *Science* **2000**, *287*, 1942.

(20) The reaction is thermodynamically favored, as shown by calculations. B–C (468 kJ/mol) and B–H (464 kJ/mol) bonds are stronger by 87 kJ/mol than B–B (434 kJ/mol) and C–H (409 kJ/mol) bonds that are broken in the reaction between B_2pin_2 and an alkane (calculations were performed with CH_4). The reaction with HBpin producing an H–H bond (434 kJ/mol) is also exothermic by 29 kJ/mol. This clearly shows why boron-containing compounds are key reagents in alkane functionalization. See: Wan, X.; Wang, X.; Luo, Y.; Takami, S.; Kubo, M.; Miyamoto, A. *Organometallics* **2002**, *21*, 3703.

(21) Webster, C. E.; Fan, Y.; Hall, M. B.; Kunz, D.; Hartwig, J. F. *J. Am. Chem. Soc.* **2003**, *125*, 858.

(22) Liu, D.; Lam, K. C.; Lin, Z. *Organometallics* **2003**, *22*, 2827.

bonded in different modes, σ -borane and dihydridoborate,¹¹ whereas when using an excess of the 9-BBN dimer a bis(dihydridoborate) complex was isolated.²³ In this article, we describe a new family of σ -borane and dihydridoborate complexes prepared by stoichiometric reactions of HBpin, HBcat, and 9-BBN with **1**. We focus on structural and theoretical studies (DFT/B3LYP) that show subtle differences between σ -borane and dihydridoborate coordination modes. These differences are not only dependent on the substituents on the boron atom, i.e., the Lewis acidity of the borane, but also on the behavior of the ancillary ligands. An understanding of how borane coordination to a metal center is controlled could be useful in understanding and improving known catalytic processes and, hopefully, in designing new ones.

Experimental Section

General Considerations. All reactions were performed using standard Schlenk or drybox techniques under argon. Solvents were dried and distilled prior to use. All reagents were purchased from Aldrich, except $\text{RuCl}_3 \cdot 3\text{H}_2\text{O}$, which came from Johnson Matthey Ltd, and were used without further purification, except HBpin and HBcat, which were purified by trap-to-trap techniques. NMR solvents were dried using appropriate methods and degassed prior to use. NMR samples of sensitive compounds were all prepared under an argon atmosphere, using NMR tubes fitted with Teflon septa. NMR spectra were recorded on Bruker AC 200 (with ^1H at 200.13 MHz and ^{31}P at 81.015 MHz), DPX 300 (with ^1H at 300.13 MHz, ^{31}P at 121.49 MHz, and ^{13}C at 75.46 MHz), and AMX 400 (with ^1H at 400.13 MHz, ^{31}P at 161.98 MHz, ^{13}C at 100.71 MHz, ^{29}Si at 79.50 MHz, ^{11}B at 128.38 MHz, and ^2H at 61.42 MHz) spectrometers. Crystal data were collected at low temperature on an Xcalibur Oxford Diffraction diffractometer, equipped with an Oxford Cryosystems cryostream cooler device and using graphite-monochromated Mo K α radiation ($\lambda = 0.71073 \text{ \AA}$). The complex $\text{RuH}_2(\eta^2\text{-H}_2)_2(\text{PCy}_3)_2$ (**1**) was prepared according to a published procedure,²⁴ and the synthesis of **3Bpin** has already been reported.¹¹

Synthesis of $\text{RuH}_2(\eta^2\text{-HBpin})(\eta^2\text{-H}_2)(\text{PCy}_3)_2$ (2Bpin**).**
Method a. Addition of HBpin (13.3 μL , 0.09 mmol) to a stirred suspension of **1** (47.2 mg, 0.07 mmol) in 0.4 mL of THF led to gas evolution and complete dissolution after 2 min. The beige solution was left at room temperature in the glovebox for crystallization. After 24 h, a mixture of colorless crystals in small quantity with a large amount of starting material was deposited in the bottom of the Schlenk tube. Unfortunately, it was not possible to separate them efficiently.

Method b. A sample of **3Bpin** dissolved in C_7D_8 was placed under an atmosphere of dihydrogen. The NMR spectra run after 5 min showed quantitative conversion to **2Bpin**.

Method c. A 20 mg portion of **1** (0.03 mmol) and 10 mg of B_2pin_2 (0.04 mmol) were placed in an NMR tube, and 0.5 mL of C_7D_8 was added. The tube was heated to 80 $^\circ\text{C}$ for 5 h. By the last two methods, NMR spectra were consistent with the formation of **2Bpin** and HBpin (which later was hydrolyzed to $(\text{Bpin})_2\text{O}$). Data for **2Bpin** are as follows. ^1H NMR (C_7D_8 , 293 K, 300.13 MHz): δ –8.83 (br, 5H, RuH_5), 1.25 (s, 12H, Bpin), 1.34–2.17 (m, 66H, PCy_3). $T_{1\rho}$ (C_7D_8 , 253 K, 300.13 MHz): 40 ms for the hydride resonance. $^{13}\text{C}\{^1\text{H}\}$ NMR (C_7D_8 , 293 K, 75.47 MHz): δ 25.1 (s, CH_3), 81.7 (s, BOC). $^{31}\text{P}\{^1\text{H}\}$

(23) Essalah, K.; Barthelat, J. C.; Montiel-Palma, V.; Lachaize, S.; Donnadieu, B.; Chaudret, B.; Sabo-Etienne, S. *J. Organomet. Chem.* **2003**, *680*, 182.

(24) Borowski, A. F.; Sabo-Etienne, S.; Christ, M. L.; Donnadieu, B.; Chaudret, B. *Organometallics* **1996**, *15*, 1427.

NMR (C_7D_8 , 293 K, 121.49 MHz): δ 72.2 (s). $^{11}B\{^1H\}$ NMR (C_7D_8 , 293 K, 96.29 MHz): δ 35.1 (br, $w_{1/2} = 509$ Hz).

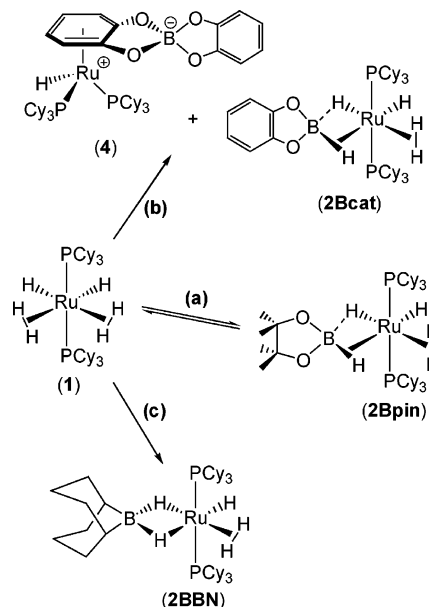
Synthesis of $RuH_2(\eta^2-HBcat)(\eta^2-H_2)(PCy_3)_2$ (2Bcat**).** Addition at room temperature of HBcat (11.5 μ L, 0.107 mmol) to a stirred suspension of **1** (57.5 mg, 0.086 mmol) in 1.1 mL of pentane resulted in immediate dihydrogen evolution and complete dissolution of the solid. A red-orange solid precipitated immediately in very small quantities and was identified as the complex $RuH(\eta^6-C_6H_4O_2BO_2C_6H_4)(PCy_3)_2$ (**4**). The filtered orange solution was kept at -36 °C until pale yellow crystals were formed (after one night). The solution was filtered off, and the crystals were dried under vacuum (32% yield). Data for **2Bcat** are as follows. 1H NMR (C_7D_8 , 293 K, 300.13 MHz): δ -8.48 (br, 5H, RuH_5), 6.95, 6.77 (m, 4H, Bcat), 1.0–2.2 (m, 66H, PCy_3). T_{1min} (C_7D_8 , 198 K, 300.13 MHz): 47 ms for the hydride resonance. $^{13}C\{^1H\}$ NMR (C_7D_8 , 293 K, 75.47 MHz): δ 152.5 (s, BOC), 120.4, 109.9 (s, Bcat). $^{31}P\{^1H\}$ NMR (C_7D_8 , 293 K, 121.49 MHz): δ 70.2 (s). $^{11}B\{^1H\}$ NMR (C_7D_8 , 293 K, 96.29 MHz): δ 35.8 (br, $w_{1/2} = 350$ Hz). Anal. Calcd for $C_{42}H_{75}O_2BP_2Ru$: C, 64.17; H, 9.63. Found: C, 64.21; H, 10.31.

Synthesis of $RuH[(\mu-H)_2BBN](\eta^2-H_2)(PCy_3)_2$ (2BBN**).** Addition of [9-BBN] $_2$ (13.8 mg, 0.056 mmol) dissolved in 1.2 mL of THF to a stirred suspension of **1** (53.4 mg, 0.080 mmol) in 0.8 mL of THF resulted in very slow but total dissolution in about 1 h. The orange solution was kept at room temperature for crystallization over 48 h. Yellow crystals of **2BBN** were obtained together with colorless crystals of 9-BBN dimer. The solution was filtered off, and **2BBN** crystals were separated manually from the others, as far as possible (less than 25% yield). Purification of the mixture using different solvents was unsuccessful. Data for **2BBN** are as follows. 1H NMR (C_7D_8 , 300.13 MHz): 293 K, δ -9.3 (vbr), 2.5–1.1 (m, C_8H_{14} and PCy_3); 253 K, δ -4.9 (br, 2H, $Ru-\mu-H_2B$), -11.48 (br t, 3H, $RuH(H_2)$). T_1 (C_7D_8 , 253 K, 300.13 MHz): 40 ms ($Ru-\mu-H_2B$), 34 ms ($RuH(H_2)$). $^{31}P\{^1H\}$ NMR (C_7D_8 , 121.49 MHz): 293 K, δ 66.0 (br); 253 K, δ 65.8 (s).

Synthesis of $RuH(\eta^6-C_6H_4O_2BO_2C_6H_4)(PCy_3)_2$ (4**).** Compound **4** was obtained by decomposition of **2Bcat** in the presence of an excess of HBcat.²⁵ Alternatively, **4** was isolated as an orange-red solid in small quantities during the synthesis of **2Bcat**. 1H NMR (C_7D_8 , 293 K, 300.13 MHz): δ -11.46 (t, $^2J_{PH} = 43.2$ Hz, 1H, RuH), 6.98, 7.31 (br, non coordinated ring), 5.07, 5.21 (br, coordinated ring), 1.1–2.1 (m, PCy_3). $^{31}P\{^1H\}$ NMR (C_7D_8 , 293 K, 121.49 MHz): δ 57.7 (s). $^{11}B\{^1H\}$ NMR (C_7D_8 , 293 K, 96.29 MHz): δ 15.7 (s).

Computational Details. DFT calculations were performed with the Gaussian 98 series of programs²⁶ using the nonlocal hybrid functional denoted as B3LYP.^{27,28} For ruthenium, the core electrons were represented by a relativistic small-core pseudopotential using the Durand–Barthelat method.²⁹ The 16 electrons corresponding to the 4s, 4p, 4d, and 5s atomic orbitals were described by a (7s, 6p, 6d) primitive set of Gaussian functions contracted to (5s, 5p, 3d). Standard pseudopotentials developed in Toulouse were used to describe the atomic cores of all other non-hydrogen atoms (C, B, O, and P).³⁰ A double plus polarization valence basis set was employed for each atom (d-type function exponents were 0.80, 0.60, 0.85, and 0.45, respectively). For hydrogen, a standard primitive (4s) basis contracted to (2s) was used. A p-type polarization function (exponent 0.9) was added for the hydrogen atoms directly bound to ruthenium. The geometry of the various

Scheme 1. Reactions of **1 with Neutral Boranes:**
(a) **1** Equiv of HBpin in THF; (b) **1.1** Equiv of HBcat in Pentane; (c) **0.5** Equiv of (9-BBN) $_2$ in THF, Benzene, or Toluene



critical points on the potential energy surface was fully optimized with the gradient method available in Gaussian 98. Calculations of harmonic vibrational frequencies were performed to determine the nature of each critical point. The NBO analysis of our complexes was not relevant. Even when appropriate methods were used to consider 3c–2e bonds and/or resonance in the Lewis structure, the highly delocalized electron density always prevented the localization of one to two valence electrons in the calculated natural orbitals. The analysis and comparison of their occupancies were then meaningless.

Results and Discussion

Synthesis and Characterization of $RuH_2(\eta^2-HBpin)(\eta^2-H_2)(PCy_3)_2$ (2Bpin**).** The stoichiometric reaction of **1** with HBpin in toluene- d_8 was followed by NMR spectroscopy. Substitution of one labile $\sigma-H_2$ ligand by one B–H bond results in an equilibrium between **1** and $RuH_2(\eta^2-HBpin)(\eta^2-H_2)(PCy_3)_2$ (**2Bpin**) at room temperature (see Scheme 1a). When using a large excess of HBpin, a new equilibrium is established between **2Bpin** and $RuH[(\mu-H)_2Bpin](\eta^2-HBpin)(PCy_3)_2$ (**3Bpin**), synthesized and characterized previously by X-ray diffraction.¹¹ These successive equilibria prevented any isolation of pure **2Bpin** in high yield. Nevertheless, NMR experiments confirm its formulation without, however, giving insights into the borane coordination mode. The 1H NMR spectrum displays in the high-field region only one broad signal at δ -8.83 , corresponding to the five hydrides in fast exchange. No decoalescence was observed, even at 183 K. The T_{1min} value of 40 ms at 253 K (300 MHz) is in agreement with the presence of a $\sigma-H_2$ ligand. Fast exchange let us anticipate that low energy barriers and low energy differences should be encountered between at least two of the three possible isomers that can be found in polyhydride species, as shown in Figure 1. The $^{11}B\{^1H\}$ NMR spectrum shows a broad signal (δ 35.1, $w_{1/2} = 509$ Hz) slightly shifted to low field compared to free HBpin (δ 28.1), in the region generally associated with σ -borane or boryl complexes.

(25) Rodriguez, A.; Sabo-Etienne, S.; Chaudret, B. *Anal. Chim. Acta* **1996**, *331*.

(26) Frisch, M. J., et al. *Gaussian 98*, revision A.11; Gaussian, Inc.: Pittsburgh, PA, 2001.

(27) Becke, A. D. *J. Chem. Phys.* **1993**, *98*, 5648.

(28) Lee, C.; Yang, W.; Parr, R. G. *Phys. Rev. B* **1988**, *37*, 785.

(29) Durand, P.; Barthelat, J. C. *Theor. Chim. Acta* **1975**, *38*, 283.

(30) Bouteiller, Y.; Mijoule, C.; Nizam, M.; Barthelat, J. C.; Daudey, J. P.; Pelissier, M.; Silvi, B. *Mol. Phys.* **1988**, *65*, 295.

Table 1. Crystal Data for the Compounds 2Bpin, 2Bcat, and 2BBN

	2Bpin	2Bcat	2BBN
formula	C ₄₂ H ₈₃ BO ₂ P ₂ Ru	C ₄₂ H ₇₅ BO ₂ P ₂ Ru	C ₄₄ H ₈₅ BP ₂ Ru
formula wt	793.90	785.84	787.94
cryst syst	monoclinic	monoclinic	orthorhombic
space group	<i>P2₁/c</i>	<i>P2₁/c</i>	<i>Pnma</i>
<i>Z</i> ; calcd density, mg/m ³	4; 1.240	4; 1.268	4; 1.101
abs coeff, mm ⁻¹	0.477	0.492	0.423
<i>F</i> (000)	1720	1688	1712
<i>a</i> , Å	10.9533(7)	23.827(4)	23.6220(13)
<i>b</i> , Å	15.9247(9)	9.8024(7)	20.4907(12)
<i>c</i> , Å	24.7405(13)	19.0158(18)	9.8244(5)
β , deg	99.786(5)	112.01(2)	90
<i>V</i> , Å ³	4252.6(4)	4117.8(8)	4755.3(5)
temp, K	90(2)	100(2)	100(2)
no. of data/restraints/params	12 972/0/457	13 559/0/453	4982/0/245
goodness of fit on <i>F</i> ²	1.102	0.927	1.112
R1 (<i>I</i> > 2 σ (<i>I</i>))	0.0270	0.0306	0.0378
wR2 (<i>I</i> > 2 σ (<i>I</i>))	0.0585	0.0625	0.0980
R1 (all data)	0.0292	0.0504	0.0391
wR2 (all data)	0.0596	0.0667	0.0989
largest diff peak and hole, eÅ ⁻³	0.697 and -0.842	1.048 and -0.525	0.355 and -1.810

The formulation of **2Bpin** as a σ -borane complex is finally ascertained by single-crystal X-ray diffraction. A first measurement at 180 K allowed the localization of all the heavy atoms and the hydrides, except those of the σ -H₂ ligand. However, a maximum of electron density accounting over one electron was found at the middle of the expected location for a σ -H₂ moiety, behavior which could be in agreement with a free rotating dihydrogen. A new X-ray diffraction experiment was then carried out at 90 K. The high quality of the data and the measurement at very low temperature, to prevent dihydrogen rotation as much as possible, allowed the location of all the hydrogen atoms around the ruthenium. Remarkably, the σ -H₂ ligand is found to be perpendicular to the equatorial plane (see Figure 3 and Tables 1 and 2). The ruthenium atom is in a pseudooctahedral environment with the phosphines in axial positions. The dihydrogen ligand is only slightly activated with a H–H distance of 0.79(3) Å. Moreover, its orientation is quite unusual for a polyhydride complex, where a stabilizing H/H₂ cis interaction resulting from

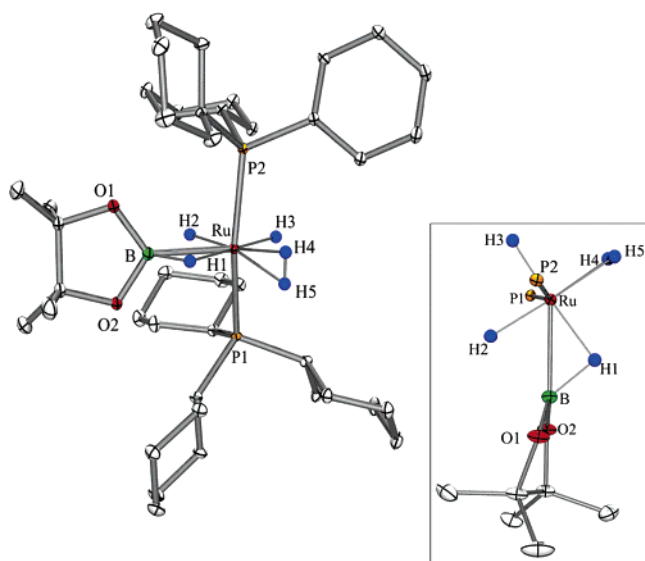


Figure 3. Structure of **2Bpin** (thermal ellipsoids set at 50% probability; protons omitted for clarity). In the framed view, the cyclohexyl groups are omitted for clarity.

Table 2. Selected Bond Lengths (Å) and Angles (deg) for 2Bpin (X-ray) and the Four Optimized Isomers of 5Bpin (DFT/B3LYP)

	2Bpin	5Bpin			
		a	b	c	d
Ru–P1	2.3525(3)	2.353	2.353	2.340	2.343
Ru–P2	2.3600(3)	2.353	2.354	2.340	2.342
Ru–B	2.173(2)	2.162	2.207	2.276	2.252
Ru–H1	1.67(2)	1.764	1.775	1.750	1.745
Ru–H2	1.57(2)	1.615	1.678	1.784	1.768
Ru–H3	1.56(2)	1.637	1.636	1.744	1.758
Ru–H4	1.71(1)	1.788	1.720	1.631	1.634
Ru–H5	1.70(3)	1.787	1.726	1.631	1.632
B–H1	1.30(2)	1.362	1.372	1.320	1.324
B···H2	1.89(2)	2.003	1.497	2.224	2.465
H4–H5	0.79(3)	0.858	0.906	0.878	0.872
B–O1	1.406(2)	1.413	1.424	1.399	1.400
B–O2	1.406(2)	1.413	1.423	1.399	1.400
Ru–H1–B	93.28(6)	86.5	88.1	94.6	93.4
Ru–B–H1	50.1(8)	54.6	53.5	50.0	50.7
Ru–H2–B	77.2(6)	72.5	87.9	68.2	61.7
B–Ru–H3	146.5(8)	143.4	130.7	93.9	83.1
B–Ru–H4	123.8(6)	126.4	156.3	164.2	160.8
P1–Ru–P2	157.66(1)	164.8	170.7	166.7	162.6
O1–B–O2	109.2(1)	109.5	109.2	110.9	110.8
H1–Ru–H2	94.7(10)	100.9	81.1	100.4	109.4
H2–Ru–H3	88.4(11)	81.3	88.1	28.8	28.6
H4–Ru–H5	26.6(10)	27.8	30.5	81.4	84.9
Cent(O1,O2)–B–Ru	170.0	165.3	173.2	162.6	161.3
ΔE (kJ/mol)		2.5	0.0	18.4	23.0

an in-plane orientation is generally expected.³¹ In our case, the perpendicular orientation seems to be preferred to avoid back-donation competition between the σ -borane and the σ -dihydrogen ligands. The B–H1 bond distance (1.30(2) Å) represents a normal elongation for a σ -borane complex by comparison to the calculated B–H bond distance of 1.17 Å in a free dialkoxyborane.³² The coordination mode adopted by the borane is clearly of a σ -borane mode, with a very small Lewis acid/base interaction between the hydride H(2) and the boron atom, as reflected by the long distance of 1.89(2) Å. Moreover, the structural data on the σ -borane dihydridoborate complex **3Bpin** give structural parameters for comparison between dihydridoborate and σ -borane

(31) Maseras, F.; Lledos, A.; Clot, E.; Eisenstein, O. *Chem. Rev.* **2000**, *100*, 601.

(32) Rablen, P. R.; Hartwig, J. F. *J. Am. Chem. Soc.* **1996**, *118*, 4648.

coordination modes.¹¹ The most convincing criterion is related to the orientation of the Bpin groups. The Bpin group in a σ -borane ligation is clearly not pointing toward the metal, as it should be in a dihydridoborate or a dihydride boryl species. The angle between the middle of [O,O], B, and Ru (170.0°) in **2Bpin** is close to the σ -borane corresponding angle (171.5°) and significantly different from the dihydridoborate angle (177.1°) in **3Bpin**. The Ru–B bond length (2.173(2) Å) is intermediate to the Ru–B distances in **3Bpin** (2.188(5) and 2.157(5) Å). Discussion on the parameters involving the different types of hydrogen atoms, hydride or σ -coordinated (dihydrogen or borane), will be found in the theoretical section.

Synthesis and Characterization of RuH₂(η^2 -HBcat)(η^2 -H₂)(PCy₃)₂ (2Bcat). The mixture of **1** with 1.1 equiv of HBcat in pentane affords colorless crystals of RuH₂(η^2 -HBcat)(η^2 -H₂)(PCy₃)₂ (**2Bcat**) isolated in 32% yield (see Scheme 1b). The rather low yield can be explained by the formation of the zwitterionic complex RuH(η^6 -C₆H₄O₂BO₂C₆H₄)(PCy₃)₂ (**4**) as a result of borane decomposition. We have reported the characterization of **4** in a previous paper.²⁵ Marder et al. have proposed a decomposition mechanism based on the presence of free phosphine.³³ NMR experiments reveal a behavior similar to that of **2Bpin**, as expected with borane reagents of the same nature. Indeed, the hydrides are all in fast exchange even at 183 K, as shown by the single broad resonance at –8.48 ppm in the ¹H NMR spectrum. The integration is in agreement with one Bcat group in the coordination sphere of the metal, and the T_{min} value of 47 ms at 198 K (300 MHz) indicates the presence of a σ -dihydrogen ligand. The ¹¹B-{¹H} NMR spectrum shows a broad signal (δ 35.8, $w_{1/2}$ = 353 Hz) shifted to low field compared to free HBcat (δ 28.8).

The σ -borane formulation for **2Bcat** is deduced from the X-ray structure determined at 100 K (see Tables 1 and 3 and the Supporting Information). The data are of good quality, but the electronic density is quite delocalized around the ruthenium center. Even if the hydrides have been located on electron density maps, analysis of their positions must be done with caution, especially regarding the orientation of the dihydrogen ligand H(4)–H(5), which could still be rotating. However, the overall structure compares well with that of **2Bpin**. The Bcat orientation is a key parameter to confirm the adoption of a dissymmetrical coordination mode: i.e., a σ -borane. Indeed, the angle Cent(O1,O2)–B–Ru is 170.3°, with Cent(O1,O2) in the equatorial plane. The Ru–B bond length of 2.124(2) Å is significantly shorter than in **2Bpin**. The better π -acceptor character of H–Bcat compared to H–Bpin is certainly responsible for a stronger Ru–B bond in that case. This trend has already been described in the literature.³

Synthesis and Characterization of RuH[(μ -H)₂-BBN](η^2 -H₂)(PCy₃)₂ (2BBN). The addition of 0.5 equiv of (9-BBN)₂ dimer to a solution of **1** in THF results in slow formation of RuH[(μ -H)₂-BBN](η^2 -H₂)(PCy₃)₂ (**2BBN**)

Table 3. Selected Bond Lengths (Å) and Angles (deg) for **2Bcat** (X-ray) and the Four Optimized Isomers of **5Bcat** (DFT/B3LYP)

	2Bcat	5Bcat			
		a	b	c	d
Ru–P1	2.3573(5)	2.357	2.358	2.345	2.348
Ru–P2	2.3335(5)	2.357	2.358	2.345	2.348
Ru–B	2.124(2)	2.135	2.198	2.231	2.208
Ru–H1	1.71(2)	1.777	1.791	1.752	1.749
Ru–H2	1.63(2)	1.615	1.693	1.792	1.766
Ru–H3	1.58(2)	1.634	1.629	1.752	1.758
Ru–H4	1.74(2)	1.789	1.713	1.632	1.633
Ru–H5	1.71(2)	1.789	1.719	1.629	1.632
B–H1	1.24(2)	1.359	1.354	1.320	1.325
B··H2	1.60(2)	1.958	1.451	2.201	2.461
H4–H5	0.77(3)	0.856	0.909	0.872	0.872
B–O1	1.443(2)	1.437	1.447	1.422	1.424
B–O2	1.444(2)	1.437	1.447	1.422	1.424
Ru–H1–B	90.6(7)	84.9	87.5	92.1	90.7
Ru–B–H1	53.7(8)	56.0	54.5	51.6	52.4
Ru–H2–B	82.3(7)	72.3	88.4	67.0	60.3
B–Ru–H3	136.1(6)	142.9	130.3	93.5	82.4
B–Ru–H4	130.5(7)	127.0	157.4	163.0	159.7
P1–Ru–P2	155.67(2)	164.1	169.8	166.7	162.2
O1–B–O2	106.4(2)	107.4	107.3	108.5	108.3
H1–Ru–H2	83.5(8)	100.7	79.3	101.3	111.3
H2–Ru–H3	88.0(8)	81.2	89.0	28.5	28.7
H4–Ru–H5	25.7(9)	27.7	30.7	82.1	85.3
Cent(O1,O2)–B–Ru	170.3	165.5	173.5	163.1	162.3
ΔE (kJ/mol)		4.6	0.0	24.0	25.0

as the main compound (see Scheme 1c). The reaction could also be performed in benzene or toluene, but was faster in THF thanks to the 9-BBN·THF adduct formation.³⁴ The successive reaction of **2BBN** with an excess of 9-BBN affords the 16-electron bis(dihydridoborate) complex Ru[(μ -H)₂BBN]₂(PCy₃) and the 9-BBN·PCy₃ adduct, as previously reported.²³ At 298 K, the ¹H NMR spectrum of **2BBN** shows fast-exchanging hydrides characterized by one broad peak at δ –9.3. Decoalescence is observed when decreasing the temperature, and two peaks appear at high field at 253 K. The broad singlet at δ –4.90 is assigned to the two bridging hydrides (B–H–Ru), whereas the terminal hydride and the σ -dihydrogen ligands, still in fast exchange even at 193 K, resonate as a broad pseudo-triplet at δ –11.48. The presence of the σ -dihydrogen is confirmed by T_1 measurements. At 253 K, the values are 40 and 34 ms, respectively (the minimum value could not be measured). The low relaxation time for the bridging hydrides is indicative of a slow exchange process, still remaining between all the hydrides at that temperature. We were not able to detect any boron signal for **2BBN** by ¹¹B-{¹H} NMR. The decoalescence phenomenon with a 2:3 ratio of the hydride signals and the well-known strong Lewis acidity of 9-BBN support a dihydridoborate coordination mode in **2BBN**.

This formulation is confirmed by X-ray analysis of a yellow monocrystal of **2BBN** at 100 K (see Figure 4 and Table 1). The ruthenium is in a pseudo-octahedral environment with the phosphines in axial positions. The cyclohexyl groups of the phosphines are oriented in order to avoid any steric hindrance with the BBN. The adopted coordination mode is thus the result of electronic effects. As expected for a dihydridoborate ligand,^{5a} the Ru–B bond is significantly longer than in **2Bpin**

(33) (a) Dai, C. Y.; Robins, E. G.; Scott, A. J.; Clegg, W.; Yufit, D. S.; Howard, J. A. K.; Marder, T. B. *J. Chem. Soc., Chem. Commun.* **1998**, 1983. (b) Westcott, S. A.; Taylor, N. J.; Marder, T. B.; Baker, R. T.; Jones, N. J.; Calabrese, J. C. *J. Chem. Soc., Chem. Commun.* **1991**, 304. (c) Westcott, S. A.; Blom, H. P.; Marder, T. B.; Baker, R. T.; Calabrese, J. C. *Inorg. Chem.* **1993**, *32*, 2175.

(34) Brown, H. C.; Kukarni, S. U. *J. Org. Chem.* **1977**, *42*, 4169.

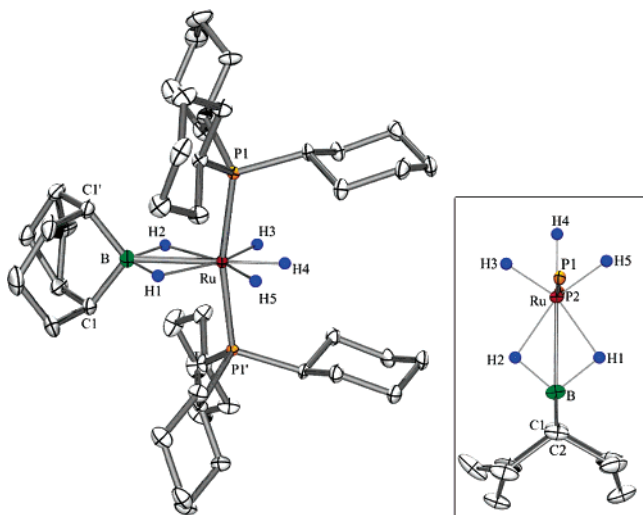


Figure 4. Structure of **2BBN** (thermal ellipsoids set at 50% probability; protons omitted for clarity). The disorder on a carbon in the BBN group has been resolved as two possible conformations. Selected bond lengths (Å) and angles (deg): Ru–P(1), 2.3502(5); Ru–B, 2.346(4); B–C(1), 1.608(3); B–H(1), 1.31(4); B–H(2), 1.34(5); P(1)–Ru–P(1'), 165.98(3); H(1)–Ru–H(2), 69(2); Cent(C1,C1')–B–Ru, 177.9.

and **2Bcat**, and its value of 2.346(4) Å is high enough to exclude a dihydride boryl coordination mode.^{6a} Moreover, the orientation of the BBN (the angle Cent(C1,C1')–B–Ru is 177.9°) agrees with a dihydridoborate coordination. This angle slightly deviates from 180°, as a result of the dissymmetry induced by the terminal hydride and the σ -H₂, both trans to the dihydridoborate. Unfortunately, the highly delocalized electronic density precluded any good location in that region of the equatorial plane trans to the dihydridoborate, and the H(3), H(4), and H(5) positions should be considered as artifacts (see below). To solve that problem, we calculated a Fourier difference map of the electronic density observed at small angles in the equatorial plane (see Figure 5 and the Supporting Information).^{35,36} After subtraction of the heavy-atom contributions, the resulting map allows a more accurate localization of the hydrogen atoms, and the elongated dihydrogen H(4)–H(3) now clearly appears. A small dissymmetry is also revealed in the dihydridoborate, in agreement with the previous observation. Even when looking at small angles, the electronic density is still very delocalized, as a result of an H/H₂ cis interaction between H(5) and H(4)–H(3). Eisenstein et al. have proved that kind of interaction to be favored by the σ -donor and π -donor abilities of a ligand such as iodine in RuHI(η^2 -H₂)(PCy₃)₂ or the carboxylate in RuH(η^2 -O₂CCH₂CH₃)(η^2 -H₂)(PCy₃)₂, for example.^{31,37,24,38} The dihydridoborate behaves in a similar manner. This interaction is also responsible for the fast exchange of the three hydrogen atoms, as observed by NMR spectroscopy.

Theoretical Studies of 2Bpin and 2Bcat: The Role of σ -H₂. The last remark about **2BBN** gives us a

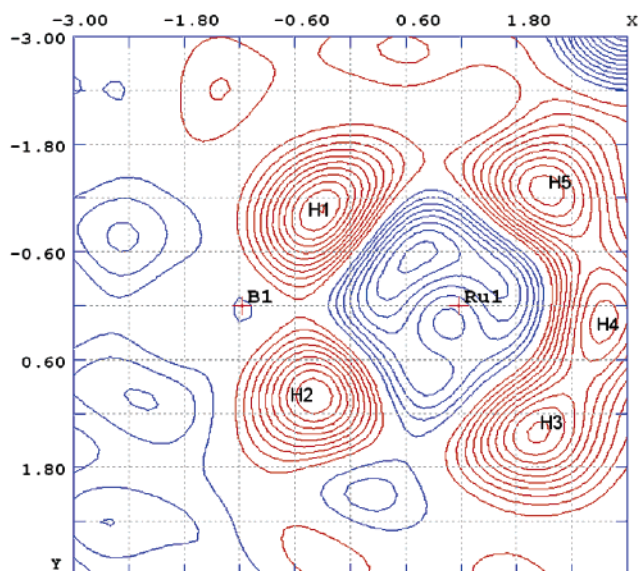


Figure 5. Fourier difference map of the experimental electronic density at small angles ($\theta = 16.5^\circ$) in the equatorial plane of **2BBN** (heavy-atom contributions have been subtracted). The atoms are localized according to the restricted density.

key to understanding why the σ -H₂ ligand is preferentially out of the equatorial plane in **2Bpin** and **2Bcat** structures. The free lone pairs of the oxygen atoms interact with the sp²-hybridized “vacant” p orbital of the boron atom in the two complexes (at some point, the effect is reduced in the Bcat analogue because of structural constraints and competing interaction with the arene ring). The interaction with the adjacent hydride H(2) is disfavored, and consequently a dihydridoborate mode and a H/H₂ cis interaction are also unfavorable. According to ¹H NMR data, the rotation of the σ -H₂ group has a low energy barrier in these complexes. What happens when the σ -H₂ ligand is in the equatorial plane? A theoretical study (DFT/B3LYP) of **2Bpin** and **2Bcat** was thus performed to address this question. RuH₅[B(OCH₂)₂](PMe₃)₂ (**5Bpin**) and RuH₅(Bcat)(PMe₃)₂ (**5Bcat**) were used as models for **2Bpin** and **2Bcat**, respectively. For each one, four isomers have been optimized as local minima on the singlet spin state potential energy surface: **5Bpin_a** and **5Bcat_a** corresponding to the X-ray structures, **5Bpin_b** and **5Bcat_b** with a dihydridoborate coordination mode, and finally, isomers with the σ -H₂ adjacent to the boron, either in the equatorial plane (**5Bpin_c** and **5Bcat_c**) or perpendicular to it (**5Bpin_d** and **5Bcat_d**). The geometries of the **5Bpin** isomers are depicted in Figure 6, and selected parameters are listed in Tables 2 and 3 for **5Bpin** and **5Bcat**, respectively.

The isomers RuH₂[η^2 -HB(OCH₂)₂](η^2 -H₂)(PMe₃)₂ (**5Bpin_a**) and RuH[(μ -H)₂B(OCH₂)₂](η^2 -H₂)(PMe₃)₂ (**5Bpin_b**) are accidentally degenerate, as their energy difference ΔE is only 2.5 kJ/mol. The same remark can be made for **5Bpin_c** and **5Bpin_d**. The optimized structural parameters of **5Bpin_a** fit well with those determined by X-ray diffraction for **2Bpin** and are in agreement with a σ -borane formulation. The angles implying the hydrides are not so well reproduced, but the trends are well represented. The difference between the calculated and experimental P(1)–Ru–P(2) angles

(35) La Placa, S. J.; Ibers, J. A. *Acta Crystallogr.* **1965**, *18*, 511.

(36) Lantero, D. R.; Ward, D. L.; Smith, M. R., III. *J. Am. Chem. Soc.* **1997**, *119*, 9699.

(37) Chaudret, B.; Chung, G.; Eisenstein, O.; Jackson, S. A.; Lahoz, F. J.; Lopez, J. A. *J. Am. Chem. Soc.* **1991**, *113*, 2314.

(38) Heyn, R. H.; Macgregor, S. A.; Nadasdi, T. T.; Ogasawara, M.; Eisenstein, O.; Caulton, K. G. *Inorg. Chim. Acta* **1997**, *259*, 5.

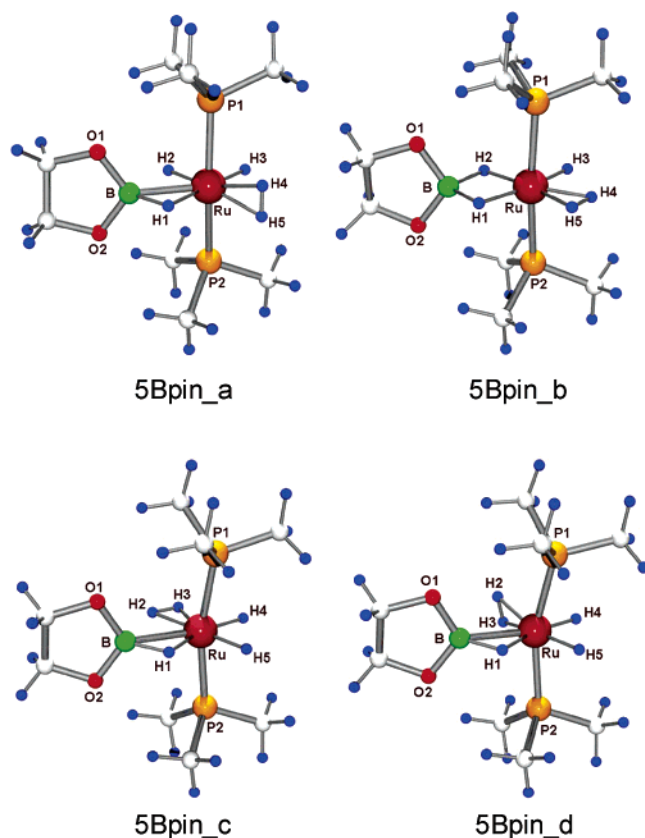


Figure 6. Representation of the four optimized isomers of **5Bpin** (DFT/B3LYP).

is the result of using PMe_3 as a model for PCy_3 . The simple rotation of the $\sigma\text{-H}_2$ ligand between **5Bpin_a** and **5Bpin_b** has a dramatic effect in the coordination mode of the borane attached ligand going from σ -borane to dihydridoborate. The latter isomer is now very similar to **2BBN**, although the hydride delocalization does not seem as important. The slight dissymmetry in the dihydridoborate (the B–H distances are 1.372 and 1.497 Å) is certainly induced by the overall dissymmetry in the equatorial plane. As expected, this change in the borane coordination mode is accompanied by an elongation of the Ru–B bond of +0.045 Å. The $\text{B}(\text{OCH}_2)_2$ group tends to be closer to the H(1)–B–H(2) bisecting plane, as shown by the $\text{Cent}(\text{O1},\text{O2})\text{-B-Ru}$ angle of 173.2° (versus 165.3° in **5Bpin_a**). This is a way to compensate back-donation competition between the H–H and B–H antibonding orbitals. The dihydridoborate mode **5Bpin_b** favors a H/H₂ cis interaction. Actually, the “dihydridoborate” formulation should be replaced by “acid/base Lewis adduct” as a better reflection of the dissymmetric situation. Such a term highlights the Lewis acidity of the borane, a key factor in these systems.

The isomers **5Bpin_c** and **5Bpin_d** are typically σ -borane complexes without any stabilizing interaction between the boron atom and the adjacent hydride. Indeed, their $\text{Cent}(\text{O1},\text{O2})\text{-B-Ru}$ angles are the smallest ones of the series. The Ru–B bonds of 2.276 and 2.252 Å, respectively, are longer than in **5Bpin_a**, as a result of a weaker coordination to the metal center. This explains why the B–O bonds (1.399 and 1.400 Å) tend to go back to their initial length of 1.372 Å calculated for $\text{HB}(\text{OCH}_2)_2$. As coordination is weakened,

the boron atom returns to an sp^2 hybridization and the B–O bonds are reinforced. We can then conclude that the energy difference between **5Bpin_b** and **5Bpin_c**, for example (18.4 kJ/mol), gives us an idea of the stabilization energy due to a H/BH interaction in our system. However, this energy difference remains small, in agreement with fast-exchanging hydrides. When we now compare **5Bpin_c** and **5Bpin_d**, the rotation of the $\sigma\text{-H}_2$ ligand let us appreciate the structural influence of the back-donation from the metal to the $\sigma^*(\text{B-H})$. While the Ru–B bond is shortened by -0.024 Å in **5Bpin_d**, thanks to a better bonding, the Ru–H(1) and B–H(1) bonds change by no more than 0.005 Å. This structural deformation related to the bond activation process has already been described for silane activation and alkane agostic interactions.^{39–41}

A similar analysis can be done for **5Bcat** isomers, thanks to their great similitude with **5Bpin**. This is not surprising, since **HBcat** and $\text{HB}(\text{OCH}_2)_2$ are of the same nature. The only subtle differences are the steric constraints due to the arene ring and the electron-withdrawing character of the latter. A slightly higher Lewis acidity for **HBcat** is expected, as the oxygen lone pairs are less willing to interact with the boron “vacant” p orbital. Unfortunately, the energy differences are again too small to discuss such a subtle difference in Lewis acidity. For the same reason, **5Bcat_a** and **5Bcat_b** are degenerate, like **5Bcat_c** and **5Bcat_d** obviously are.

Our attempts to reproduce a similar theoretical study on the **2BBN** complex led to an unexpected result. The calculations gave, as expected, a dihydridoborate structure^{5d} but also the same wrong positions for H3, H4, and H5 deriving from the X-ray data before analysis at small angles. This comforts our idea that these hydrides are delocalized, as a result of a strong H/H₂ cis interaction. The potential energy surface is then certainly too flat to support an arrested structure, with a terminal hydride and a $\sigma\text{-H}_2$ ligand in the equatorial plane, as a local minimum. No isomer with an out-of-plane $\sigma\text{-H}_2$ could be optimized. It is indeed noteworthy that this theoretical study of **2BBN** leads to the same conclusion about proton delocalization as that deduced from NMR and X-ray data. The frontier between a Ru(IV) and Ru(II) species appears not to be so well delimited.

Theoretical Study of 3Bpin. The complex $\text{RuH}[(\mu\text{-H})_2\text{Bpin}](\eta^2\text{-HBpin})(\text{PCy}_3)_2$ (**3Bpin**) was previously characterized by X-ray and NMR studies.¹¹ It was the first complex displaying two boron-attached ligands coordinated to the same metal center with different coordination modes, a σ -borane and a dihydridoborate. The geometry of $\text{RuH}[(\mu\text{-H})_2\text{B}(\text{OCH}_2)_2][\eta^2\text{-HB}(\text{OCH}_2)_2](\text{PMe}_3)_2$ (**6Bpin_a**) optimized at the DFT/B3LYP level provides a good agreement with the **3Bpin** X-ray structure (see Figure 7 and Table 4). The hydrides H(3) and H(4) are slightly different, for the same reasons invoked in the case of **5Bpin_b**. No bis(σ -borane) isomer was found on the potential energy surface. Since H–Bpin is similar to H–H in terms of π -acceptor ability, it leads to an important competition for back-donation that results in the formation of a strong Lewis acid/base

(39) Schubert, U. *Adv. Organomet. Chem.* **1990**, *30*, 151.

(40) Crabtree, R. H. *Angew. Chem., Int. Ed. Engl.* **1993**, *32*, 789.

(41) Crabtree, R. H.; Holt, E. M.; Lavin, M. E.; Morehouse, S. M. *Inorg. Chem.* **1985**, *24*, 1986.

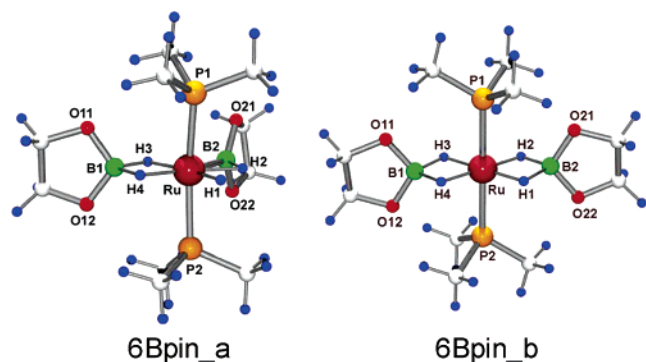


Figure 7. Representation of the two optimized isomers of **6Bpin** (DFT/B3LYP).

Table 4. Selected Bond Lengths (Å) and Angles (deg) for **3Bpin (X-ray) and the Two Optimized Isomers of **6Bpin** (DFT/B3LYP)**

	3Bpin	6Bpin	
		a	b
Ru–P1	2.367(2)	2.364	2.414
Ru–P2	2.357(2)	2.365	2.413
Ru–B1	2.188(5)	2.234	2.205
Ru–B2	2.157(5)	2.159	2.195
Ru–H1	1.48(3)	1.636	1.703
Ru–H2	1.58(3)	1.685	1.708
Ru–H3	1.49(3)	1.762	1.715
Ru–H4	1.55(3)	1.709	1.709
B2–H2	1.35(3)	1.394	1.447
B2···H3	2.09(3)	2.487	3.678
B1–H3	1.58(3)	1.389	1.439
B1–H4	1.47(3)	1.426	1.436
B1–O11	1.415(5)	1.423	1.426
B1–O12	1.392(6)	1.424	1.417
B2–O21	1.383(5)	1.402	1.418
B2–O22	1.396(5)	1.402	1.427
B1–Ru–B2	113.7(2)	116.4	179.1
Ru–B2–H2	47(2)	51.3	51.0
Ru–B1–H3	43(2)	52.0	51.0
Ru–B1–H4	45(2)	49.9	50.8
B1–Ru–H3	46(2)	38.4	41.2
B1–Ru–H4	42(2)	39.6	41.3
B2–Ru–H2	39(2)	40.2	40.7
B2–Ru–H3	67(2)	78.0	139.7
P1–Ru–P2	160.45(3)	169.0	179.3
O11–B1–O12	109.2(4)	109.3	108.4
O21–B2–O22	110.0(3)	110.3	108.4
H1–Ru–H2	81(2)	73.9	81.3
H1–Ru–H4	85(2)	89.8	97.2
Cent(O11,O12)–B1–Ru	177.1	176.4	177.7
Cent(O21,O22)–B2–Ru	171.5	168.1	177.7
ΔE (kJ/mol)		0.0	16.0

adduct, assimilated to a dihydridoborate. In contrast, we could optimize the geometry of the bis(dihydridoborate) isomer $\text{Ru}[(\mu\text{-H})_2\text{B}(\text{OCH}_2)_2]_2(\text{PMe}_3)_2$ (**6Bpin_b**). The ruthenium center is in an octahedral environment, and the Ru–B bonds (2.205 and 2.195 Å) are very similar to that in **5Bpin_b** (2.207 Å). In comparison to the latter, the ligands display a symmetrical dihydridoborate arrangement. This isomer is, however, at significantly higher energy than **6Bpin_a** ($\Delta E = 16.0$ kJ/mol). The exo isomer **6Bpin_a** is thus preferred, in agreement with the X-ray structure of **3Bpin**.

It is noteworthy that borane substitution by H_2 in **3Bpin** is fast and quantitative, leading to **2Bpin**. In contrast, substitution of the σ -borane ligand in **2Bpin** by H_2 , leading back to **1**, is a much lower process: 15 min to go from **3Bpin** to **2Bpin**, whereas around 1000

min is required to regenerate **1** from **2Bpin** under 1 bar of H_2 . Interestingly, the lability of the σ ligands can be used to catalyze the conversion of HBpin into DBpin under 1 bar of D_2 .⁴²

Conclusion

Combination of NMR and X-ray data with theoretical studies is invaluable in establishing the coordination mode of borane reagents to a metal fragment, a problem that is difficult to solve in highly fluxional systems. Caution should always be taken to avoid any conclusion based on artifacts that can be present on such delocalized species. We have fully characterized three new borane complexes resulting from the stoichiometric reaction of **1** with HBpin, HBcat, and 9-BBN. The coordination mode adopted by the borane simultaneously reflects the Lewis acidity of the borane reagent and the Lewis basicity of the polyhydride ruthenium fragment. The dialkoxyborane ligands (HBpin and HBcat) are not acidic enough to stabilize a “true” symmetrical dihydridoborate mode. They thus lead to σ -borane complexes presenting a small H/BH cis interaction between the boron atom and the adjacent hydride H(2). Such a H/BH cis interaction obviously depends on the Lewis basicity of H(2) but also reflects the subtle change in the boron acidity, as shown by the theoretical study. When the in-plane position of the $\sigma\text{-H}_2$ ligand imposes a competition for back-donation, the H/BH cis interaction is reinforced, resulting in an unsymmetrical dihydridoborate mode also described as a strong Lewis acid/base adduct. Remarkably, $\sigma\text{-H}_2$ rotation and σ -borane versus dihydridoborate ligation are intimately correlated. The 9-BBN reagent is, in contrast, a strong Lewis acid and leads to a dihydridoborate complex. This ligand induces such a high delocalization of the trans hydrides that only an in-depth study of the experimental electron density allowed us to differentiate the terminal hydrides from the $\sigma\text{-H}_2$ ligand. Finally, one can notice that the symmetry of the borane coordination mode is dependent on the symmetry of the coordination sphere of the metal, and the inverse is true. However, the theoretical study of **3Bpin** shows that the bonding is also dependent on the hydride basicity. The $\text{RuH}[(\mu\text{-H})_2\text{B}(\text{OCH}_2)_2](\text{PMe}_3)_2$ fragment is not basic enough to form a second dihydridoborate ligand, despite the stabilization that should be gained from the resulting symmetrical structure. This study highlights the role of the borane Lewis acidity on their behavior as ligand and especially on the H/BH cis interaction in our systems. The role of the ancillary ligands is also crucial, since they determine the hydride basicity and the overall symmetry of the coordination sphere of the metal.

These results on borane activation are reminiscent of the σ -ligand substitution mechanism some of us already proposed in silane chemistry,⁴³ in which the same kind of cis interaction between hydrides and silicon (SISHA interaction) plays a key role. Keeping

(42) Callaghan, P. L.; Fernandez-Pacheco, R.; Jasim, N.; Lachaize, S.; Marder, T. B.; Perutz, R.; Rivalta, E.; Sabo-Etienne, S. *Chem. Commun.* **2004**, 242.

(43) Atheaux, I.; Delpech, F.; Donnadiou, B.; Sabo-Etienne, S.; Chaudret, B.; Hussein, K.; Barthelat, J. C.; Braun, T.; Duckett, S. B.; Perutz, R. N. *Organometallics* **2002**, *21*, 5347.

in mind the problem of alkane and arene functionalization, our borane complexes could serve as models for a σ -bond metathesis step between Ru–H and B–H bonds. Theoretical investigations on the corresponding transition states are in progress. Efforts to establish the significance of mechanisms involving σ -bonds and weak secondary interactions in catalysis are currently underway.

Acknowledgment. This work is supported by the CNRS. We thank the CINES (Montpellier, France) for a generous allocation of computer time. S.L. thanks the

French Ministry “Education Nationale, Enseignement Supérieur, Recherche” for his AMN grant. We also thank Dr. Jean-Claude Daran for assistance with the X-ray studies.

Supporting Information Available: Tables and figures giving complete crystallographic details for $\text{RuH}_2(\eta^2\text{-HBpin})(\eta^2\text{-H}_2)(\text{PCy}_3)_2$ (**2Bpin**), $\text{RuH}_2(\eta^2\text{-HBcat})(\eta^2\text{-H}_2)(\text{PCy}_3)_2$ (**2Bcat**), and $\text{RuH}[(\mu\text{-H})_2\text{BBN}](\eta^2\text{-H}_2)(\text{PCy}_3)_2$ (**2BBN**) and optimized geometries of all species and calculated energies. This material is available free of charge via the Internet at <http://pubs.acs.org>.

OM050276L